



How biomass growth mode affects ammonium oxidation start-up and NOB inhibition in the partial nitrification of cold and diluted reject water

V. Kouba, P. Svehla, M. Catrysse, L. Prochazkova, H. Radechovska, P. Jenicek & J. Bartacek

To cite this article: V. Kouba, P. Svehla, M. Catrysse, L. Prochazkova, H. Radechovska, P. Jenicek & J. Bartacek (2019) How biomass growth mode affects ammonium oxidation start-up and NOB inhibition in the partial nitrification of cold and diluted reject water, Environmental Technology, 40:6, 673-682, DOI: [10.1080/09593330.2017.1403491](https://doi.org/10.1080/09593330.2017.1403491)

To link to this article: <https://doi.org/10.1080/09593330.2017.1403491>



Published online: 21 Nov 2017.



Submit your article to this journal [↗](#)



Article views: 68



View Crossmark data [↗](#)



Citing articles: 1 View citing articles [↗](#)



How biomass growth mode affects ammonium oxidation start-up and NOB inhibition in the partial nitrification of cold and diluted reject water

V. Kouba^a, P. Svehla^b, M. Catrysse^c, L. Prochazkova^a, H. Radechovska^b, P. Jenicek^a and J. Bartacek^a

^aDepartment of Water Technology and Environmental Engineering, University of Chemistry and Technology, Prague, Czech Republic;

^bDepartment of Agro-Environmental Chemistry and Plant Nutrition, Czech University of Life Sciences Prague, Prague, Czech Republic;

^cDepartment of Biosystems Engineering, Ghent University, Ghent, Belgium

ABSTRACT

The inhibition of undesirable nitrite oxidizing bacteria (NOB) and desirable ammonium oxidizing bacteria (AOB) by free ammonia (FA) and free nitrous acid (FNA) in partial nitrification (PN) is crucially affected by the biomass growth mode (suspended sludge, biofilm, encapsulation). But, the limitations of these modes towards less concentrated reject waters (≤ 600 mg-N L⁻¹) are unclear. Therefore, this work compares the start-up and stability of three PN sequencing batch reactors (SBRs) with biomass grown in one of the three modes: suspended sludge, biofilm and biomass encapsulated in polyvinyl alcohol (PVA) pellets. The SBRs were operated at 15°C with influent total ammonium nitrogen (TAN) concentrations of 75–600 mg-TAN L⁻¹. PN start-up was twice as fast in the biofilm and encapsulated biomass SBRs than in the suspended sludge SBR. After start-up, PN in the biofilm and suspended sludge SBRs was stable at 150–600 mg-TAN L⁻¹. But, at 75 mg-TAN L⁻¹, full nitrification gradually developed. In the encapsulated biomass SBR, full nitrification occurred even at 600 mg-TAN L⁻¹, showing that NOB in this set-up can adapt even to 4.3 mg-FA L⁻¹ and 0.27 mg-FNA L⁻¹. Thus, PN in the biofilm was best for the treatment of an influent containing 150–600 mg-TAN L⁻¹.

ARTICLE HISTORY

Received 19 May 2017

Accepted 23 October 2017

KEYWORDS

Partial nitrification; suspended sludge; biofilm; encapsulated biomass; ammonium oxidizing bacteria and nitrite oxidizing bacteria

Introduction

Partial nitrification (PN) has recently gained attention in the context of partial nitrification-anammox for the removal of nitrogen from carbon-deprived wastewaters, particularly nitrogen-rich streams [1,2] and anaerobically pre-treated sewage [3]. Compared with conventional nitrification-denitrification, this approach reduces the consumption of oxygen for aeration, the requirement for a denitrification electron donor and the production of excess activated sludge [4,5]. For these beneficial reasons, PN is currently applied to reject water and to specific industrial streams with total ammonium nitrogen (TAN) concentrations higher than 600 mg-N L⁻¹ at temperatures above 25°C [6]. In sequencing-batch reactors (SBRs), such high TAN concentrations and high pH at cycle start selectively inhibit undesirable nitrite oxidizing bacteria (NOB) by free ammonia (FA). Subsequently, the oxidation of ammonium to nitrite by ammonium oxidizing bacteria (AOB) consumes alkalinity and reduces pH, thus inhibiting NOB by free nitrous acid (FNA) [7–9].

However, NOB may be inhibited less efficiently by FA and FNA in reject waters that are less concentrated (≤ 600 mg-TAN L⁻¹) and colder ($\leq 25^\circ\text{C}$), both of which

they often are. The temperature of reject water decreases primarily under storage in winter conditions in mild climates. And the concentration of TAN in reject water decreases based on local conditions, such as the content of dry matter in raw sludge, chemical composition of raw sludge, conditions applied during anaerobic digestion, and efficiency of the anaerobic digestion process. Also, some industrial wastewaters have TAN concentrations in the range of 100–600 mg L⁻¹ (e.g. fertilizer manufacturing [10] and food industry [11]). Furthermore, new concepts of wastewater treatment, such as direct anaerobic treatment in the main stream, can increase TAN concentration in wastewater by releasing TAN previously bound in proteins [3,12]. Under these lower temperatures and at these concentrations, what constitutes an approximate lower TAN threshold suitable for PN in treated wastewater is not currently known.

The inhibition of bacteria is driven by their exposure to inhibitors, which is strongly dependent on the biomass growth mode used (e.g. suspended sludge, biofilm and encapsulation) [13,14]. However, studies of the inhibition/adaptability of AOB and NOB to FA and FNA generally only assess one type of biomass growth

mode: suspended sludge [7,15–23], biofilm [24–28], granules [29–31] or encapsulated biomass [32,33]. In some such studies, this assessment has been somewhat clouded by the use of an additional mechanism for the selective inhibition of NOB, such as dissolved oxygen (DO) limitation [18] or real-time cycle control [34]. Moreover, it is well known that the resulting inhibition of AOB and NOB can be affected by variations in the following key factors: (i) important substrate characteristics (e.g. C/N ratio [35], phosphorus [36] and trace elements such as Cu [37] and Fe [38]); (ii) operational parameters, such as SRT [35]; (iii) pre-exposure of the biomass to inhibitors enabling adaptation; (iv) temperature-altering AOB and NOB growth rate [39], as well as the speciation of ammonium ($\text{NH}_3/\text{NH}_4^+$) and nitrite ($\text{HNO}_2/\text{NO}_2^-$) [40]; and (v) the bacterial species in the AOB and NOB microbial communities [41]. Collectively, this all makes it very difficult to draw firm conclusions from the existing literature about the optimal biomass growth mode for the selective inhibition of NOB by FA and FNA.

To enhance understanding of how biomass growth mode affects the susceptibility of AOB and NOB to FA and FNA inhibition, this study used nitrifying cultures cultivated in the form of suspended sludge, biofilm and biomass encapsulated in polyvinyl alcohol (PVA) pellets. These cultures, operated in three separate SBRs, received diluted reject water from anaerobic digestion. The different biomass growth modes were assessed for the sensitivity of AOB to FA during start-up and, with the aim of identifying the lowest TAN concentration enabling PN application, for the efficiency of NOB inhibition by FA and FNA at gradually reduced influent TAN concentrations (600–75 mg-N L⁻¹). The SBRs were operated under the same parameters, thereby minimizing the effect of other potential AOB and NOB inhibitors. Furthermore, the potential growth rate of AOB and NOB was equalized by setting the operational temperature to 15°C. These conditions enabled us to compare the three biomass growth modes for the treatment of low-nitrogen-loaded cold reject water. The applicability of our findings to the treatment of medium to low-strength industrial wastewaters and of anaerobically pre-treated sewage with limited alkalinity was also considered.

Materials and methods

Reactor setup

Experiments were performed in three fully automated lab-scale SBRs (suspended sludge, biofilm and encapsulated biomass; schematic displayed in Figure 1) operated at 15°C. The suspended sludge and biofilm SBRs were inoculated with fully nitrifying activated sludge from

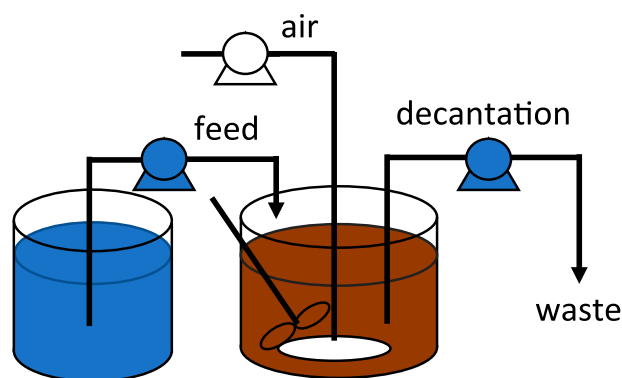


Figure 1. Schematic of SBRs used in the present study.

the central municipal wastewater treatment plant (WWTP) in Prague. The activated sludge process at this WWTP was operated as simultaneous nitrification-denitrification with a separate oxalic regeneration tank receiving reject water and return activated sludge from the clarifiers. The inoculation of the encapsulated biomass is described below.

The SBR cycle comprised a filling phase followed by an aerobic reaction phase. For each influent TAN concentration, the length of the reaction phase was adjusted to achieve a constant nitrogen loading rate of 0.2 kg-TAN m⁻³ d⁻¹. The hydraulic retention times were 3, 1.5, 0.75 and 0.375 days for influent TAN concentrations of 600, 300, 150 and 75 mg-TAN L⁻¹, respectively. The length of the settling phase was 30 min for the suspended sludge SBR and 10 min for the biofilm and encapsulated biomass SBRs; in all cases, this was followed by a decanting phase. Air supply was provided by air diffusers placed at the bottom of the reactors. To prevent the potential inhibition of AOB and NOB, the DO concentration exceeded 3.0 mg-O₂ L⁻¹ throughout the entire cycle in all SBRs [42]. The pH in the reactors was not externally controlled, changes in pH simply reflecting biochemical and/or physico-chemical changes. The alkalinity of the influent water was not artificially improved. Certain differences in the volumes the SBRs were caused by the different methods of biomass cultivation.

To determine the lowest influent TAN concentration necessary to induce efficient inhibition, the study started with 600 mg-TAN L⁻¹. After achieving constant TAN conversion (ca. 50%), stable operation of the SBRs at 600 mg-TAN L⁻¹ was initiated for a period of time. Subsequently, the influent nitrogen concentrations in the suspended sludge and biofilm SBRs were stepwise reduced to 300, 150 and 75 mg-TAN L⁻¹. At each concentration, these two reactors were operated for at least 35 days in order to verify the stability of the process under the given conditions.

Suspended sludge SBR

This SBR had a working volume of 1.5 L. To ensure the maximum amount of AOB in the system, no excess sludge was withdrawn [43].

Biofilm SBR

As a biomass carrier, this SBR used biomass-free lens-shaped PVA pellets (LentiKat's Biocatalyst) with a diameter of 3–4 mm and a thickness of 0.2–0.3 mm. The working volume of this SBR was 0.78 L [44].

Encapsulated biomass SBR

The working volume of this SBR was 1 L. PVA pellets (LentiKat's Biocatalyst) with a diameter of 3–4 mm and a thickness of 0.2–0.3 mm were used during the experiments up to a total weight of 150 g. These pellets contained a mixture of *Nitrosomonas europaea* and *Nitrobacter winogradskyi*. Inoculation to immobilize these bacteria was performed by LentiKat's (Prague, Czech Republic). The pellets were manufactured by mixing dissolved PVA with a minimum amount of polyethylene glycol and bacterial suspension. The mixture was dropped on an appropriate surface and dried by airflow using a temperature gradient of 40–30°C. During the drying, polymer gelation took place and a porous structure was formed inside the pellets. Subsequently, a solution of sodium sulfate was added to stabilize the pellets and, thereby, strengthen the PVA structure [45]. PVA MOWIOL 28-99 (Kuraray America, Inc.) with a 99% degree of saponification and relative molecular mass of 145,000 g mol⁻¹ was used for immobilization [33]. The start-up of the encapsulated biomass SBR was performed by adding the inoculated pellets.

Wastewater

Reject water from anaerobic digestion was diluted with tap water to obtain influent TAN concentrations of 600, 300, 150 and 75 mg-TAN L⁻¹, and used as the media. In this way, low-nitrogen-loaded reject water, specific industrial wastewaters and anaerobically pre-treated municipal wastewater were simulated. The reject water was obtained from the full-scale digester of Prague's central WWTP operated at a stable temperature of 55°C as shown in Jenicek et al. [46]. Each start-up was performed with an influent TAN concentration of 600 mg-TAN L⁻¹.

The most important influent wastewater parameters are displayed in Table 1. The key average parameters of the raw reject water were as follows: 1.25 g-TAN L⁻¹; alkalinity 64 mmol L⁻¹; 2.3 g-COD L⁻¹; soluble COD concentration of 1.1 g-COD L⁻¹; total solids 3.6 g-TS L⁻¹; and total suspended solids 1.15 g-TSS L⁻¹.

Table 1. Parameters of influent wastewater fed into SBRs.

Parameter/Period (mg-TAN L ⁻¹)	600	300	150	75
TAN (mg L ⁻¹)	585±15	297±7	145±19	77±7
COD, total (mg L ⁻¹)	1200±300	830±220	410±130	130±31
COD, soluble (mg L ⁻¹)	490±19	280±15	170±21	75±32
pH	8.3±0.2			
Alkalinity (mmol L ⁻¹)	32	14	8	4.4
Alkalinity/TAN	0.77	0.66	0.77	0.80

Analytical methods

The concentrations of N - NO₂⁻, N - NO₃⁻, TAN as the sum of N - NH₃ and N - NH₄⁺, COD and volatile suspended solids in samples of the bulk liquid, influent and effluent were determined according to APHA [47]. Temperature and pH were analyzed using an Inolab pH 730 probe (WTW, Weilheim, Germany). The concentration of DO was measured using a Oxi 340 probe (WTW, Weilheim, Germany).

The kinetic tests used to assess the development of nitrogen species and pH during the SBR cycles were done by sampling the reactor liquid during regular operation.

The concentrations of FA and FNA were calculated according to Ford et al. using Equations (1) and (2), respectively [40]:

$$c_{FA} = \frac{17}{14} \cdot \frac{c_{TAN} \cdot 10^{pH}}{\exp\left(\frac{6334}{273 + ^\circ C}\right) + 10^{pH}}, \quad (1)$$

$$c_{FNA} = \frac{46}{14} \cdot \frac{c_{NO_2-N}}{\exp\left(\frac{-2300}{273 + ^\circ C}\right) \cdot 10^{pH}}, \quad (2)$$

The nitrite accumulation ratio (NAR) was calculated using Equation (3):

$$NAR = \frac{c_{NO_2-N}}{c_{NO_3-N} + c_{NO_2-N}}. \quad (3)$$

Results and discussion

Start-up of PN

During start-up, the TAN concentration in each reactor was 370 ± 120 mg L⁻¹, while pH ranged from 7.8 to 9.2 depending on actual AOB activity in the respective SBR cycle. At a constant temperature of 15°C, the FA concentrations ranged from 5.3 to 180 mg-FA L⁻¹. In the start-up period, such high FA content led to the stripping of ammonia and, consequently, TAN losses between the effluent and influent of 39 ± 18% (Figure 2). The intensity of AOB activity was an important factor in determining the actual pH in the reactor and, in turn, the concentrations of FA and FNA. This activity is accompanied by

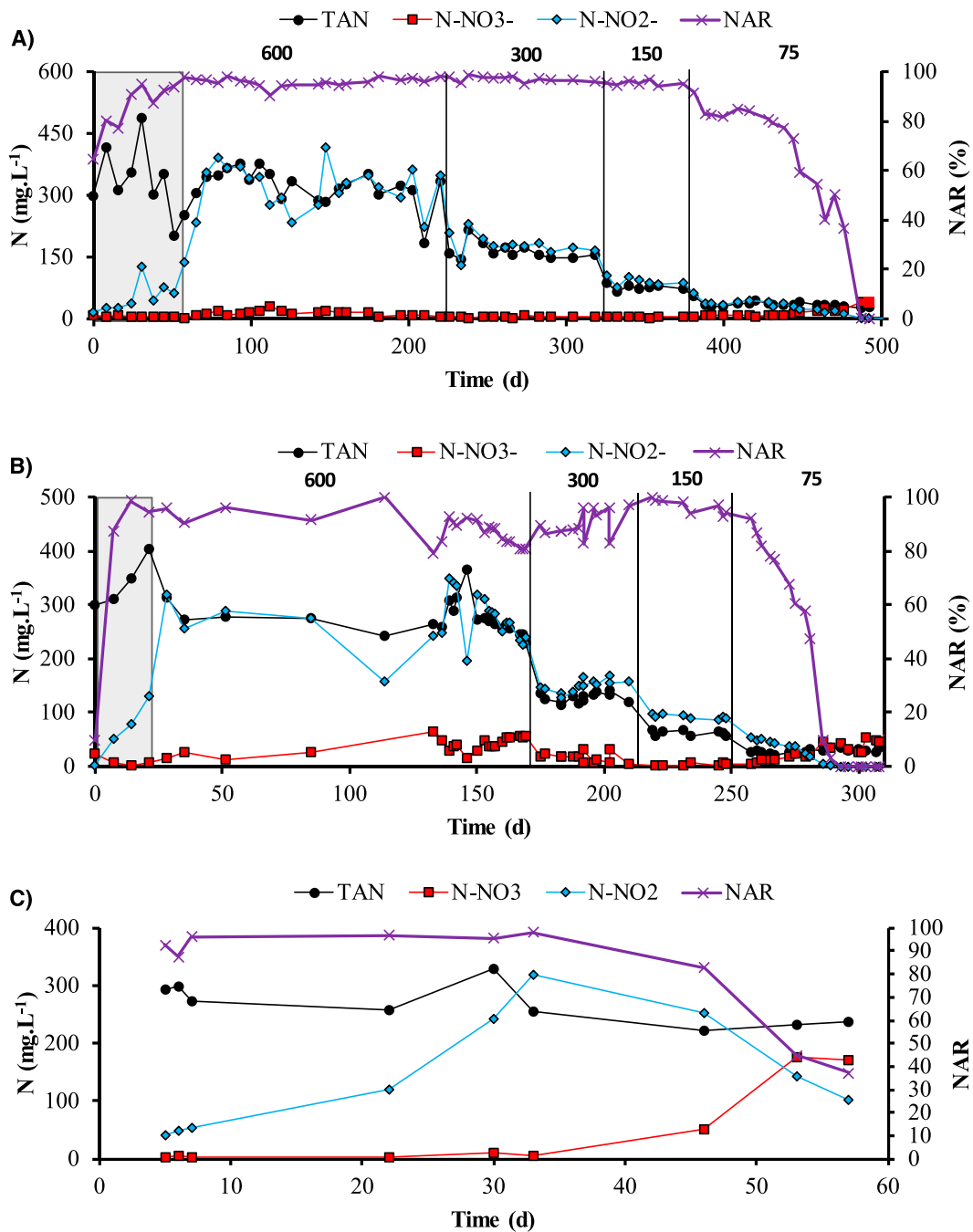


Figure 2. Start-up and PN in suspended sludge (A), biofilm (B) and encapsulated biomass (C) SBRs for the influent TAN concentrations of 600, 300, 150 and 75 mg-TAN L⁻¹. Influent nitrogen concentration in encapsulated biomass SBR was 600 mg-TAN L⁻¹ during the entire experiment. NAR is nitrite accumulation ratio ($N - NO_2^- / N - NO_x$). Start-up period of SBRs is indicated by rectangle at the beginning of operation.

H⁺ production and pH decrease. Therefore, during start-up, AOB activity (as well as H⁺ production) was limited, resulting in a high pH and a high FA concentration. The gradual increase in AOB activity during start-up resulted in a gradual decrease in both pH and FA. This explains the wide range of FA up to extremely high values (5.3–180 mg) obtained during start-up.

For suspended, biofilm and encapsulated biomass SBRs, the respective representations of N - NO₂⁻ in oxidized nitrogen (NAR = $N - NO_2^- / N - NO_x$) were 92 ±

10%, 95 ± 38% and 96 ± 4%, showing that the activity of NOB was successfully inhibited during start-up.

The main objective at start-up was to obtain a maximum conversion of TAN to N-NO_x of ~50%. The achievement of this conversion was intrinsically limited by the alkalinity available in the substrate, or more precisely, by the ratio alkalinity:TAN concentration (Table 1) [20]. Such conversion was observed after one month for the biofilm and encapsulated biomass SBRs, and after two months for the suspended sludge SBR (Figure 2).

Considering the identical conditions in all SBRs and the absence of conventional AOB inhibitors, such as DO limitation, PN start-up was most likely limited by the inhibition of AOB by high concentrations of FA.

The above-reported FA concentrations (5.3–180 mg-FA L⁻¹) correspond to the conventional threshold (10–100 mg-FA L⁻¹) for the inhibition of AOB in nitrifying sludge reported by Anthonisen et al. [7]. Wang et al. [30] reported that AOB in granular sludge adapted to 5–10 mg-FA L⁻¹ after 35 days. In contrast, Vadivelu et al. [48] showed that neither the anabolic nor the catabolic process of enriched *Nitrosomonas* was inhibited up to 16 mg-NH₃-N L⁻¹. And interestingly, numerous researchers have demonstrated that AOB can adapt to much higher FA concentrations. For example, Hellinga et al. [49] and Van Hulle et al. [50] demonstrated that AOB cultivated in SHARON were not inhibited by 70–300 mg-NH₃-N L⁻¹.

Given that the primary inhibitor of AOB was FA, our results suggest that suspended sludge SBRs are more susceptible to such inhibition. This is very likely due to the enhanced contact of AOB with FA in this SBR compared with the biofilm or encapsulated biomass SBRs, in which the FA inhibition of AOB is limited by diffusion [51].

Stability of PN

Stable PN in the biofilm and suspended sludge SBRs at medium TAN concentration

At the medium TAN concentrations of 150–600 mg-TAN L⁻¹, the PN in the biofilm and suspended sludge SBRs was stable (NAR = 80–99%) for 8 and 10 months,

respectively (Figure 2). After start-up, the alkalinity:TAN ratio (0.66–0.80), which determines the intensity of pH decrease during PN, induced a stable 50% TAN conversion to N - NO₂⁻ (data not shown). This ratio remained largely constant throughout all operational periods (Table 1), thereby inducing relatively stable TAN conversion efficiency. Simultaneously, this stable ratio meant that the actual FA and FNA concentrations reached in the biofilm and suspended sludge SBRs were influenced much more strongly by the influent TAN concentration than by the intensity of AOB activity (see *Start-up of PN*).

The TAN conversion efficiency achieved fits the anammox stoichiometry presented by Lotti et al. [52]. However, the PN effluent pH (5.5–6.5) fell outside the anammox ecological niche of 6.7–8.3, and was significantly lower than the optimum of 8 [53]. Therefore, the use of such PN effluent in subsequent anammox would require pH adjustment. In contrast to the biofilm and suspended sludge SBRs, the encapsulated biomass SBR exhibited a gradual conversion of nitrite to nitrate that reduced the NAR from 85% to 37% in the 24 days following start-up.

In the absence of other NOB-inhibiting factors, such as limited oxygen [42] or biomass retention time limitation at high temperatures [39], it is clear that the sole NOB inhibitors in our study were FA and FNA (Figure 3). This is in accordance with Park and Bae [9], who modeled the kinetics of biochemical ammonia and nitrite oxidation simultaneously inhibited by FA and FNA. Their model indicated that the complete removal of TAN can be achieved by high nitrite accumulation in SBRs treating high-nitrogen-loaded wastewater.

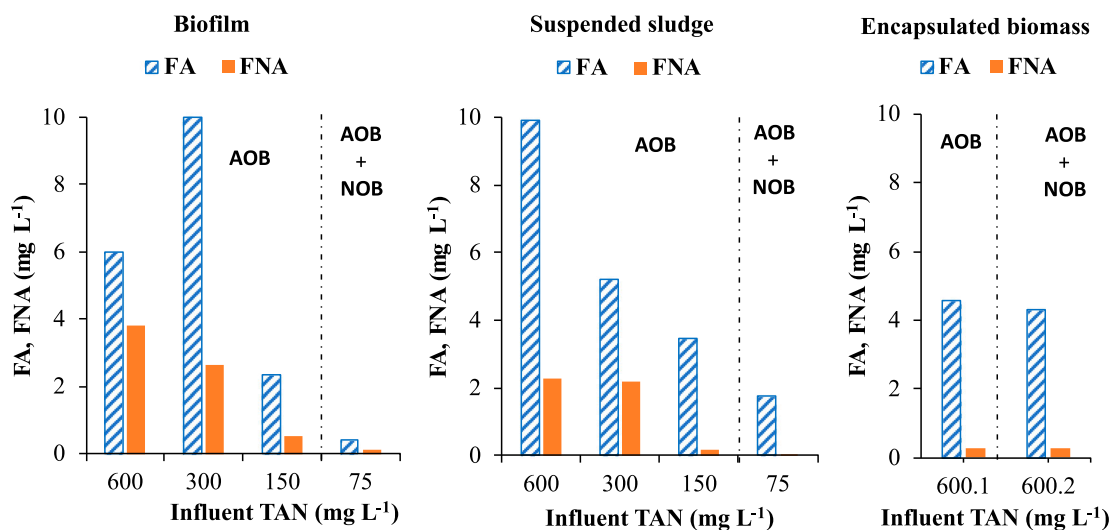


Figure 3. Concentrations of FA and FNA at the beginning and end of cycle in PN SBR, respectively, using biofilm (days 141, 183, 245 and 273), suspended sludge (days 126, 297, 346 and 463) and encapsulated biomass (days 33 and 53). Lower FA for biofilm SBR at 600 compared with 300 mg-TAN L⁻¹ is due to 1-h sampling delay in the test with 600 mg-TAN L⁻¹, first samples otherwise taken 2 min after the start of new aerobic phase.

FA and FNA toxicity in the SBR cycle

Compared with start-up, significantly lower FA concentrations were observed during the stable operation of the reactors, due to AOB activity being relatively stable (see above) by this point. The induction of FA and FNA toxicity was based on a principle illustrated using the biofilm SBR operated at an influent TAN concentration of 150 mg-TAN L⁻¹ (operational day 237) as an example. At the start of the aerobic phase of its cycle, the combination of the influent TAN concentration (150 mg-TAN L⁻¹) and average pH of 7.9 resulted in an FA concentration of 2.8 mg-FA L⁻¹ (Figure 4). The conversion of ammonium to nitrite decreased the pH to 5.8 and FA to 0.02 mg L⁻¹, the latter being compensated by an increased FNA of up to 1.21 mg-FNA L⁻¹ (Figure 4).

As shown in Figure 3, the influent TAN concentrations of 150–600 mg-TAN L⁻¹ induced initial, in other words highest FA concentrations in the ranges of 2.5–10 and 3.5–9.9 mg-FA L⁻¹ in the biofilm and suspended sludge SBRs, respectively. In both cases, FA and FNA concentrations mostly increased with influent TAN, and the inconsistencies can be attributed either to delayed sampling or to the variations of influent pH (8.3 ± 0.2). The respective highest FNA concentrations were 1.0–2.7 and 0.16–2.3 mg-FNA L⁻¹. These concentrations were similar to or higher than the widely accepted NOB inhibition thresholds for FA and FNA (1.5–10 mg-FA L⁻¹ and

0.011 mg-FNA L⁻¹, respectively) [23]. Therefore, it is not surprising that at influent concentrations of 150–600 mg-TAN L⁻¹, the production of nitrate was efficiently suppressed (Figure 2).

When the influent TAN concentration was reduced to 75 mg-TAN L⁻¹, the maximum FA concentrations reached during the cycle decreased to only 0.42 and 1.76 mg-FA L⁻¹ for the suspended sludge and biofilm SBRs, respectively. Their respective FNA concentrations at cycle end were 0.13 and 0.061 mg-FNA L⁻¹. Although these FA concentrations were similar to and even lower than the lowest inhibition thresholds, they were still expected to inhibit NOB [23]. Instead, NOB proliferation and activity was observed even at these FNA concentrations. This suggests that in our study the FNA threshold for the inhibition of NOB was above the generally accepted value of 0.011 mg-HNO₂-N L⁻¹ [23].

Slow NOB development in suspended sludge SBR at TAN concentration of 75 mg-TAN L⁻¹

For 50 days after the influent TAN concentration was reduced to 75 mg-TAN L⁻¹, the suspended sludge SBR continued to show stable PN. Over the following 100 days, NOB activity was gradually initiated (N - NO₃⁻ concentration reached 42.5 mg L⁻¹ on day 487 at NAR reaching 0.3% (Figure 2). By comparison, full nitrification was already taking place in the biofilm SBR 45 days after reduction to 75 mg-TAN L⁻¹. The longer time needed for NOB development in the suspended sludge SBR can be explained by the more efficient exposure of NOB to FA in suspended sludge [51].

Unstable PN in encapsulated biomass SBR

After the end of the start-up phase (day 33), nitrate concentration in the effluent of the encapsulated biomass SBR gradually increased (Figure 2). This indicates that NOB activity increased despite the high influent TAN concentration (600 mg-TAN L⁻¹), which induced maximum FA and FNA concentrations during SBR cycle of 4.3 mg-FA L⁻¹ and 0.27 mg-FNA L⁻¹, respectively (Figure 3). Conversely, in the suspended sludge and biofilm SBRs, NOB activity was fully inhibited even under lower concentrations (2.36 and 3.47 mg-FA L⁻¹; 0.51 and 0.14 mg-FNA L⁻¹; Figures 3 and 4). Because the influent TAN remained at 600 mg-TAN L⁻¹ for the whole period of the encapsulated biomass SBR experiment, it is likely that NOB adapted to both FA and FNA.

Villaverde et al. [54] reported the adaptation of *Nitrobacter* sp. to FA in the biofilm. Over the course of six months, they observed that the threshold for specific inhibition increased from 0.2 to 0.7 mg-FA L⁻¹. Under the given conditions of our study, NOB adapted to 4.6 mg-FA L⁻¹ in a shorter period (two months). In a

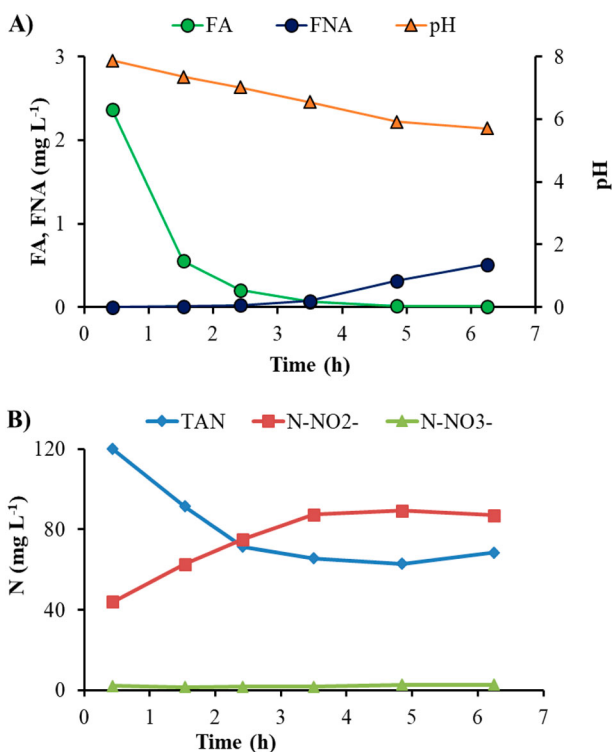


Figure 4. Profiles of FA/FNA concentrations and pH value for cycle of biofilm SBR cycle with 150 mg-TAN L⁻¹.

more extreme example, Li et al. [26] reported NOB in the biofilm adapted to even higher FA concentrations of 30–32.5 mg-FA L⁻¹.

In terms of adaptation to FNA, the literature reports significantly lower inhibition thresholds than the 0.27 mg-FNA L⁻¹ obtained for NOB cultivated in our encapsulated biomass SBR. Generally, Anthonisen et al. [7] concluded that NOB in suspended sludge are inhibited from 0.01 mg-FNA L⁻¹. Prakasam and Loehr [55] report a threshold value for NOB inhibition of 0.07 mg-FNA L⁻¹. Even lower inhibition thresholds were reported by Vadivelu et al. [56], who showed that 0.02 mg-HNO₂-N L⁻¹ totally inhibited the biosynthesis of enriched *Nitrobacter* suspended sludge, but did not affect its energy production capabilities. Other experiments with NOB in suspended sludge have suggested that the growth of NOB starts to be inhibited at 0.01 mg-FNA L⁻¹ before stopping at 0.02 mg-FNA L⁻¹ [56]. Consequently, to our best knowledge, the current study is the first to report the adaptation of NOB to as much as 0.27 mg-FNA L⁻¹.

Compared to the biofilm and suspended sludge, NOB washout from the PVA-gel pellets was less efficient. This is because such pellets are specifically designed to retain bacteria for the treatment of industrial wastewaters with high concentrations of inhibitory compounds (e.g. diphenylguanidine manufacturing, uranium mining residues). This retention is enhanced by a highly porous carrier body and surface pore size of 4.8–10.5 µm. These factors ensure that while individual cells may escape (the dimensions of *Nitrobacter winogradskyi* range from 0.4 to 1.0 µm [57]), the washout of bacterial clusters [58] is prevented. In turn, this enables the active NOB situated inside the pellets to survive even when there are relatively high FA and FNA concentrations in the reactor.

Unstable suspended sludge SBR due to biomass washout

While feeding influent with the highest TAN concentration of 600 mg-TAN L⁻¹, the amount of biomass in the suspended sludge SBR increased from 0.35 to 0.9 g-VSS L⁻¹ (Figure 5). At lower TAN concentrations of 300 and 150 mg-TAN L⁻¹, the biomass decreased to 0.40 and 0.23 g-VSS L⁻¹, respectively. This is due to the lower hydraulic retention times necessary to maintain stable nitrogen loading rates at these TAN concentrations. At 75 mg-TAN L⁻¹, the biomass concentration in the liquid decreased to 0.07 g-VSS L⁻¹ while a significant portion of the active biomass remained attached to the reactor walls.

The dramatic reduction of suspended sludge was most likely caused by unrestricted biomass washout. At a stable temperature and nitrogen loading rate, the

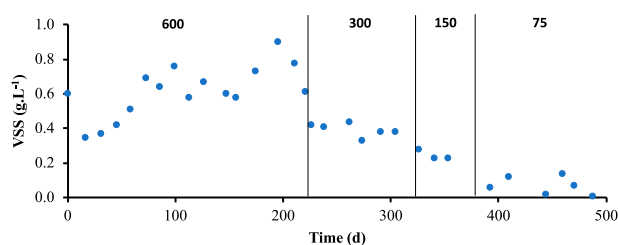


Figure 5. Concentration of VSS in suspended sludge SBR with influent TAN of 600, 300, 150 and 75 mg-TAN L⁻¹.

lowest TAN of 75 mg-TAN L⁻¹ corresponded to the shortest hydraulic retention time of 0.375 day [59]. In addition, the heterotrophic floc-forming bacteria lacked the carbon necessary to form compact flocs (loading rate 270 ± 62 kg-COD m⁻³ d⁻¹, removal rate 81 ± 26 kg-COD m⁻³ d⁻¹), due to the limited biodegradability of organic carbon in diluted reject water. As a result, the decomposed flocs were decanted in the effluent, leading to the formation of biofilm on the reactor walls. In the future, the separation properties could be enhanced by adding FeCl₃ or organic polymer.

TAN conversion and its limitation by alkalinity

After start-up, a steady TAN conversion of around 50% was achieved for suspended sludge and biofilm at the TAN concentration ranges of 150, 300 and 600 mg-N L⁻¹ (Figure 2A and B, Table 1). TAN conversion was limited by the available alkalinity in diluted reject water. PN consumed alkalinity, which resulted, by the end of the suspended sludge and biofilm SBR cycles, in a decrease of pH to 5.5–6.5 (Figure 4); in accordance with Jenicek et al. [60], this stopped AOB activity.

Implications for PN applied to low-nitrogen-loaded streams

Our results suggest that biofilm is the optimal biomass growth mode for PN in SBRs operated at medium TAN influent concentrations (150–600 mg L⁻¹) and low temperatures. In this way, they can contribute to the design of systems for removing nitrogen from low-nitrogen-loaded cold reject waters. Simultaneously, they can be used for the optimization of nitrogen removal from specific industrial wastewater streams (e.g. food industry 90–120 mg L⁻¹ of Total Kjeldahl's Nitrogen [11], fertilizer production – 6–1700 mg-TAN L⁻¹ [10,61]) and potentially even from anaerobically pre-treated municipal wastewaters with TAN concentrations above 150 mg L⁻¹ and of limited alkalinity. Furthermore, these results confirm that a long-term decrease in the feed TAN concentration below 150 mg L⁻¹ may destroy the

PN process and, thus, make it impossible to apply the subsequent anammox process. In such cases, an additional strategy for NOB inhibition, such as DO limitation [18] or real-time cycle control [34], must be applied. Another key factor affecting the efficiency of FA and/or FNA inhibition is the buffering capacity of the treated water, which determines not only the intensity of pH fluctuation during the SBR cycle, but also the FA and FNA concentrations actually achieved in the reactor.

Under the given conditions of our experiments, the suspended sludge tended to be washed out completely. Although increased risk of NOB activity was observed for the encapsulated biomass SBR, the stability of PN in such an SBR could be improved by the immobilization of an AOB enrichment culture without the presence of NOB. Additional research is needed to confirm or disprove this hypothesis.

Due to NOB adaptation to high levels of FA [54,62], Vadivelu et al. [22] hypothesized that after using high FA levels to wash out NOB at start-up, a high FNA concentration is the key to strengthening NOB inhibition. Our study supports this hypothesis by demonstrating the importance of FNA as an NOB inhibitor at the influent TAN concentrations 150–600 mg-TAN L⁻¹ and low temperature (15°C).

Conclusion

The present study has shown that the immobilization of biomass (biofilm, encapsulation) accelerates the start-up of PN in SBRs operated under the given conditions. It has also demonstrated that suspended sludge and biofilm can sustainably produce nitrite at influent TAN concentrations ranging from 150 to 600 mg-TAN L⁻¹ even without being limited by low DO or with other inhibiting mechanism. On the other hand, biomass encapsulation in PVA pellets dramatically increased the adaptability of NOB to toxic nitrogen species (FA, FNA), thereby jeopardizing the stability of PN even at 600 mg-TAN L⁻¹. This makes clear the radical differences between AOB and NOB activity in the biomass cultivated in different growth modes (suspension, biofilm, encapsulated in PVA pellets) in PN reactors applied as the preliminary stage of the anammox process. Biofilm appears to be the most stable growth mode for the treatment of cold reject water and of specific industrial wastewaters because it enables more efficient biomass retention in the reactor. Conversely, because of the risk of NOB recovery, no tested variant was able to ensure the application of PN to the treatment of anaerobically pre-treated municipal wastewaters or other streams with TAN concentrations of lower than approx. 150 mg L⁻¹. This

could only be achieved by applying additional inhibitory effect such as limitation of NOB growth by low DO.

Disclosure Statement

No potential conflict of interest was reported by the authors.

Funding

This research was funded by European Commission grant ERG-2010-268417 'Biofilms in Bioreactors for Advanced Nitrogen Removal from Wastewater (BioNIT)' and by Ministerstvo Školství, Mládeže a Tělovýchovy [MSM 6046137308]. The authors also gratefully acknowledge the support given by the Ministry of Agriculture of the Czech Republic under NAZV project No. QK1710176. Financial support from specific university research (MSMT No 20/2015) is acknowledged. This work also supported by Czech University of Life Sciences Prague [CIGA 20142028].

References

- [1] Ge S, Wang S, Yang X, et al. Detection of nitrifiers and evaluation of partial nitrification for wastewater treatment: a review. *Chemosphere*. 2015;140:85–98.
- [2] Ma B, Wang S, Cao S, et al. Biological nitrogen removal from sewage via anammox: recent advances. *Bioresource Technol*. 2016;200:981–990.
- [3] Hendrickx TLG, Wang Y, Kampman C, et al. Autotrophic nitrogen removal from low strength waste water at low temperature. *Water Res*. 2012;46:2187–2193.
- [4] Daigger GT. Oxygen and carbon requirements for biological nitrogen removal processes accomplishing nitrification, nitrification, and anammox. *Water Environ Res*. 2014;86:204–209.
- [5] Schaubroeck T, De Clippeleir H, Weissenbacher N, et al. Environmental sustainability of an energy self-sufficient sewage treatment plant: improvements through DEMON and co-digestion. *Water Res*. 2015;74:166–179.
- [6] Lackner S, Gilbert EM, Vlaeminck SE, et al. Full-scale partial nitrification/anammox experiences - An application survey. *Water Res*. 2014;55:292–303.
- [7] Anthonisen AC, Loehr RC, Prakasam TBS, et al. Inhibition of nitrification by ammonia and nitrous acid. *J Water Pollut Control Fed*. 1976;48:835–852.
- [8] Svehla P, Bartacek J, Pacek L, et al. Inhibition effect of free ammonia and free nitrous acid on nitrite-oxidising bacteria during sludge liquor treatment: influence of feeding strategy. *Chem Pap*. 2014;68:871–878.
- [9] Park S, Bae W. Modeling kinetics of ammonium oxidation and nitrite oxidation under simultaneous inhibition by free ammonia and free nitrous acid. *Process Biochem*. 2009;44:631–640.
- [10] Patwardhan A. *Industrial wastewater treatment*. Delhi: PHI Learning Pvt. Ltd.; 2017.
- [11] Qasim W, Mane AV. Characterization and treatment of selected food industrial effluents by coagulation and adsorption techniques. *Water Resour Ind*. 2013;4:1–12.
- [12] Vela JD, Stadler LB, Martin KJ, et al. Prospects for biological nitrogen removal from anaerobic effluents during

- mainstream wastewater treatment. *Environ Sci Technol Lett.* **2015**;2:234–244.
- [13] Anderson GG, O'Toole GA. Innate and induced resistance mechanisms of bacterial biofilms. *Bacterial Biofilms.* **2008**;322:85–105.
- [14] Lewis K. Persister cells and the riddle of biofilm survival. *Biochemistry-Moscow.* **2005**;70:267–274.
- [15] Qiao S, Matsumoto N, Shinohara T, et al. High-rate partial nitrification performance of high ammonium containing wastewater under low temperatures. *Bioresource Technol.* **2010**;101:111–117.
- [16] Sun H, Peng Y, Shi X. Advanced treatment of landfill leachate using anaerobic–aerobic process: organic removal by simultaneous denitrification and methanogenesis and nitrogen removal via nitrite. *Bioresource Technol.* **2015**;177:337–345.
- [17] Wei D, Du B, Xue X, et al. Analysis of factors affecting the performance of partial nitrification in a sequencing batch reactor. *Appl Microbiol Biotechnol.* **2014**;98:1863–1870.
- [18] Wei D, Du B, Zhang J, et al. Composition of extracellular polymeric substances in a partial nitrification reactor treating high ammonia wastewater and nitrous oxide emission. *Bioresource Technol.* **2015**;190:474–479.
- [19] Wei D, Xue X, Yan L, et al. Effect of influent ammonium concentration on the shift of full nitrification to partial nitrification in a sequencing batch reactor at ambient temperature. *Biochem Eng J.* **2014**;235:19–26.
- [20] Jeníček P, Švehla P, Záborská J, et al. Factors affecting nitrogen removal by nitrification/denitrification. *Water Sci Technol.* **2004**;49:73–79.
- [21] Sun H LÜX, Peng Y, Wang S, et al. Long-term nitrification performance of ammonium-rich landfill leachate. *Chin J Chem Eng.* **2015**;23:1888–1893.
- [22] Vadivelu VM, Keller J, Yuan Z. Effect of free ammonia on the respiration and growth processes of an enriched *Nitrobacter* culture. *Water Res.* **2007**;41:826–834.
- [23] Vadivelu VM, Yuan Z, Fux C, et al. The inhibitory effects of free nitrous acid on the energy generation and growth processes of an enriched *Nitrobacter* culture. *Environ Sci Technol.* **2006**;40:4442–4448.
- [24] Yamamoto T, Takaki K, Koyama T, et al. Novel partial nitrification treatment for anaerobic digestion liquor of swine wastewater using swim-bed technology. *J Biosci Bioeng.* **2006**;102:497–503.
- [25] Trapani D D, Bella G D, Mannina G, et al. Effect of C/N shock variation on the performances of a moving bed membrane bioreactor. *Bioresource Technol.* **2015**;189:250–257.
- [26] Li S, Chen Y-P, Li C, et al. Influence of free ammonia on completely autotrophic nitrogen removal over nitrite (CANON) process. *Appl Biochem Biotechnol.* **2012**;167:694–704.
- [27] Antileo C, Roeckel M, Lindemann J, et al. Operating parameters for high nitrite accumulation during nitrification in a rotating biological nitrifying contactor. *Water Environ Res.* **2007**;79(9):1006–1014.
- [28] Bae H, Yang H, Chung Y-C, et al. High-rate partial nitrification using porous poly (vinyl alcohol) sponge. *Bioprocess Biosyst Eng.* **2014**;37:1115–1125.
- [29] Yang S-F, Tay J-H, Liu Y. Inhibition of free ammonia to the formation of aerobic granules. *Biochem Eng J.* **2004**;17:41–48.
- [30] Wang F, Xia S-q, Yi L, et al. Community analysis of ammonia and nitrite oxidizers in start-up of aerobic granular sludge reactor. *J Environ Sci.* **2007**;19:996–1002.
- [31] Kim D-J, Seo D. Selective enrichment and granulation of ammonia oxidizers in a sequencing batch airlift reactor. *Process Biochem.* **2006**;41:1055–1062.
- [32] Isaka K, Yoshie S, Sumino T, et al. Nitrification of landfill leachate using immobilized nitrifying bacteria at low temperatures. *Biochem Eng J.* **2007**;37:49–55.
- [33] Vacková L, Stloukal R, Wanner J. The possibility of using encapsulated nitrifiers for treatment of reject water coming from anaerobic digestion. *Water Sci Technol.* **2012**;65:1428–1434.
- [34] Sun H, Peng Y, Wang S, et al. Achieving nitrification at low temperatures using free ammonia inhibition on *Nitrobacter* and real-time control in an SBR treating landfill leachate. *J Environ Sci.* **2015**;30:157–163.
- [35] Regmi P, Miller MW, Holgate B, et al. Control of aeration, aerobic SRT and COD input for mainstream nitrification/denitrification. *Water Res.* **2014**;57:162–171.
- [36] de Vet WWJM, van Loosdrecht MCM, Rietveld LC. Phosphorus limitation in nitrifying groundwater filters. *Water Res.* **2012**;46:1061–1069.
- [37] Wagner FB, Nielsen PB, Boe-Hansen R, et al. Copper deficiency can limit nitrification in biological rapid sand filters for drinking water production. *Water Res.* **2016**;95:280–288.
- [38] Lees H, Meiklejohn J. Trace elements and nitrification. *Nature.* **1948**;161:398–398.
- [39] Hellings C, Schellen AAJC, Mulder JW, et al. The Sharon process: An innovative method for nitrogen removal from ammonium-rich waste water. *Water Sci Technol.* **1998**;37:135–142.
- [40] Ford DL, Churchwell RL, Kachtick JW. Comprehensive analysis of nitrification of chemical-processing wastewaters. *J Water Pollut Con F.* **1980**;52:2726–2746.
- [41] Blackburne R, Vadivelu VM, Yuan Z, et al. Kinetic characterisation of an enriched *Nitrospira* culture with comparison to *Nitrobacter*. *Water Res.* **2007**;41:3033–3042.
- [42] Guo J, Peng Y, Wang S, et al. Long-term effect of dissolved oxygen on partial nitrification performance and microbial community structure. *Bioresource Technol.* **2009**;100:2796–2802.
- [43] Švehla P, Radechovsky J, Hrnčířová H, et al. Effect of influent nitrogen concentration on feasibility of short-cut nitrification during wastewater treatment in activated sludge systems. *Chem Pap.* **2015**;69:921–929.
- [44] Kouba V, Catryse M, Stryjova H, et al. The impact of influent total ammonium nitrogen concentration on nitrite-oxidizing bacteria inhibition in moving bed biofilm reactor. *Water Sci Technol.* **2014**;69:1227–1233.
- [45] Novák L, Stloukal R, Rosenberg M. inventors Způsob odstraňování dusíkatého znečištění z pitných, užitkových a odpadních vod. Czech Republic patent CZ 2004-438 A3. 2004 March 30.
- [46] Jeníček P, Kutil J, Benes O, et al. Energy self-sufficient sewage wastewater treatment plants: Is optimized anaerobic sludge digestion the key? *Water Sci Technol.* **2013**;68:1739–1743.
- [47] APHA. Standard methods for the examination of water & wastewater. 21st ed. Washington (DC): Amer Public Health Assn; **2005**.

- [48] Vadivelu VM, Keller J, Yuan Z. Effect of free ammonia and free nitrous acid concentration on the anabolic and catabolic processes of an enriched *Nitrosomonas* culture. *Biotechnol Bioeng*. 2006;95:830–839.
- [49] Hellinga C, Van Loosdrecht M, Heijnen J. Model based design of a novel process for nitrogen removal from concentrated flows. *Math Comput Model Dyn Syst*. 1999;5:351–371.
- [50] Van Hulle SW, Volcke EI, Teruel JL, et al. Influence of temperature and pH on the kinetics of the Sharon nitrification process. *J Chem Technol Biotechnol*. 2007;82:471–480.
- [51] Park S, Bae W, Rittmann BE. Multi-Species Nitrifying Biofilm Model (MSNBM) including free ammonia and free nitrous acid inhibition and oxygen limitation. *Biotechnol Bioeng*. 2010;105:1115–1130.
- [52] Lotti T, Kleerebezem R, Lubello C, et al. Physiological and kinetic characterization of a suspended cell anammox culture. *Water Res*. 2014;60:1–14.
- [53] Kartal B, Keltjens JT, Jetten MSM. Metabolism and genomics of anammox Bacteria. In: Ward B, Arp D, Klotz M, editors. *Nitrification*. Washington (DC): ASM Press; 2011. p. 181–200.
- [54] Villaverde S, Fdz-Polanco F, Garcí'a PA. Nitrifying biofilm acclimation to free ammonia in submerged biofilters. Start-up influence. *Water Res*. 2000;34:602–610.
- [55] Prakasam T, Loehr R. Microbial nitrification and denitrification in concentrated wastes. *Water Res*. 1972;6:859–869.
- [56] Vadivelu V, Keller J, Yuan Z. Free ammonia and free nitrous acid inhibition on the anabolic and catabolic processes of *Nitrosomonas* and *Nitrobacter*. *Water Sci Technol*. 2007;56:89–97.
- [57] Zavarzin G, Legunkova R. The morphology of *Nitrobacter winogradskyi*. *Microbiology*. 1959;21:186–190.
- [58] Boušková A, Mrákota J, Stloukal R, et al. Three examples of nitrogen removal from industrial wastewater using *Lentikats* Biotechnology. *Desalination*. 2011;280:191–196.
- [59] Galí A, Dosta J, van Loosdrecht MCM, et al. Two ways to achieve an anammox influent from real reject water treatment at lab-scale: partial SBR nitrification and SHARON process. *Process Biochem*. 2007;42:715–720.
- [60] Jenicek P, Svehla P, Zabranska J, et al. Factors affecting nitrogen removal by nitrification/denitrification. *Water Sci Technol*. 2004;49(5–6):73–79.
- [61] Bhandari VM, Sorokhaibam LG, Ranade VV. Industrial wastewater treatment for fertilizer industry—A case study. *Desalin Water Treat*. 2016;57:27934–27944.
- [62] Wong-Chong GM, Loehr RC. Kinetics of microbial nitrification: nitrite-nitrogen oxidation. *Water Res*. 1978;12:605–609.